

# Drug Repurposing and High-throughput screening against Phosphomannomutase for the treatment of Cutaneous Leishmaniasis

Malik Nasibullah (✉ [malik@iul.ac.in](mailto:malik@iul.ac.in))

Integral University <https://orcid.org/0000-0002-4413-0515>

Sabahat Yasmeen Sheikh

Integral University

Firoj Hassan

Integral University

Mohammad Faheem Khan

Era's Lucknow Medical College and Hospital

Tanveer Ahamad

Era's Lucknow Medical College and Hospital

Waseem Ahmad Ansari

Era's Lucknow Medical College and Hospital

Yusuf Akhter

Babasaheb Bhimrao Ambedkar University

Abdul Rahman Khan

Integral University

---

## Research Article

**Keywords:** Drug Repurposing, Phosphomannomutase, Amastigote, Promastigotes, Amphotericin B, Miltefosine

**Posted Date:** April 26th, 2022

**DOI:** <https://doi.org/10.21203/rs.3.rs-1283812/v1>

**License:** © ⓘ This work is licensed under a Creative Commons Attribution 4.0 International License.

[Read Full License](#)

---

# Abstract

Cutaneous leishmaniasis (CL) is caused by the protozoan parasite *L. maxicana* is one of the major parasitic diseases throughout the world. Due to the lack of approved vaccines against CL, chemotherapy is the only modern treatment. These treatments have some major consequences including prolonged treatment, parenteral administration, tolerability, teratogenicity, etc. Presently, none of the current CL drugs have high levels of efficacy. Thus, the development of new and safer drugs possessing cost-effective, efficacious, oral and short course drugs is urgently needed. Drug repurposing is another method that can be used for the development of new therapeutic activities. When a new therapeutic activity would have been identified, the entities could be rapidly advanced into clinical trials. Phosphomannomutase (PMM) has become highlighted as potential drug targets due to its important role in the biosynthesis of glycoconjugates. These glycoconjugates are essential for parasite virulence. To identify new promising lead molecules, we have picked 8500 approved drugs for their potential to be repurposed for CL. The library of approved drugs was obtained from Zinc data-base and PMM structure (PDBID: -2i54) was retrieved from protein data bank and used for molecular docking simulation and protein-ligand interaction analysis. The protein structure was validated by the Procheck Ramachandran plot. The virtual screening of the full library of drugs by AutoDock Vina version PyRx 0.8 and selected 46 drug molecules and docking simulations were performed through Glide module of Schrodinger software. Saquinavir and Grazoprevir showed the highest binding affinity -10.144 and -10.131 kcal/mole respectively, was repurposed to be promising drug candidates for CL. To find the stability of complexes (saquinavir-2i54 and grazoprevir-2i54) were performed 100ns molecular dynamics simulation. In the molecular dynamics simulation trajectories of both complexes were analyzed. The results of grazoprevir-2i54 and saquinavir-2i54 complex were showed good stability in the active site of receptor. In conclusion, grazoprevir and saquinavir could be the alternative drugs for the treatment of CL.

## 1. Introduction

Leishmaniasis is caused by the protozoan parasite of the 20 *Leishmania* species and transmitted through the bite of female phlebotomine sandfly species.<sup>1,2</sup> During its life cycle, the parasite switches from a promastigote flagellate form within the sandfly to an intracellular amastigote form in the macrophages of the mammalian host.<sup>3</sup> It is included among 13 neglected tropical parasitic diseases by the World Health Organization Tropical Disease Research (WHO TDR).<sup>4</sup> The disease mainly strikes the poor and is associated with malnutrition, population displacement, poor housing, and a weak immune system. This disease is recognized into the three most variable forms, such as Cutaneous Leishmaniasis (CL), Mucocutaneous Leishmaniasis (ML) and Visceral Leishmaniasis (VL). CL is the most common form, recognized as skin scratches, stigma, ulcers, and scars. This disease is mostly distributed in America, the Mediterranean Basin, the Central and Middle East Asia. In September 2021, CL occurred in 56 endemic countries reported by WHO Global Leishmaniasis programme for 2020. In 2020, about 80% of global CL was reported from 7 countries (Afghanistan, Algeria, Colombia, Iraq, Pakistan, Serbia and Arab Republic). It is estimated that 6,00,000 to 1 million new cases are reported worldwide annually.<sup>5</sup> There are

two important ways to affect the development of the parasite within the host, considering proteins expressed in the amastigote form as therapeutic targets. The first one targeting proteins in biochemical pathways is leading to altered metabolism and is harmful for the parasite.<sup>6-9</sup> Another one is to avoid macrophage-parasite which plays a pivotal role on glycoconjugate recognition. Inhibition of glycoconjugate biosynthesis diminishes parasite load. The glycosylation is a key pathway for macrophage infection.<sup>10-14</sup>

Mannose is a nutritional supplement and responsible for the biosynthesis of glycoconjugates such as Glycosylphosphatidylinositol (GPI), Lipophosphoglycan (LPG), Proteophosphoglycans (PPG) and Glycoinositolphospholipid (GIPLS) which are present at the surface of the eukaryotic cell and involved in many biological processes like intercellular recognition, adhesion or signaling.<sup>15,16</sup> These glycoconjugates are essential for parasite virulence.<sup>11,14</sup> PMM is a chief therapeutic target that plays an essential role in the survival of the parasite in the mammalian life cycle.<sup>17</sup> In the mannosylation pathway, the PMM converts mannose-6-phosphate into mannose-1-phosphate which plays a crucial role in the synthesis of glycoconjugates. Hereby, the glycosylation process plays the main role in macrophage infection. PMM is an important target for the development of new drugs against *L. mexicana*.<sup>18</sup>

Pentavalent antimonials have been used for decades against CL, due to adverse side effects like musculoskeletal pain, gastrointestinal disturbances and mild to moderate headache cannot be used frequently. The current treatment options are liposomal amphotericin B, miltefosine, fluconazole and ketoconazole. These treatments have serious issues including prolonged treatment, parenteral administration, tolerability, teratogenicity etc. Now a day, none of the current CL drugs have high levels of efficacy. Thus, the development of new and safer drugs having cost-effective, efficacious, oral and short course drugs for CL is urgently needed.

Drug repurposing is an alternate method for the development of new drugs. Approved drugs have known pharmacokinetics and safety profiles.<sup>19,20</sup> When a new biological activity has been identified, the drug can be rapidly advanced into clinical trials. Here, we have selected 8500 approved drugs for their potential to be repurposed for CL.

## 2. Methods

### 2.1 Target preparation and validation

The 3D structures of PMM (PDBID:-2i54) were downloaded from Protein Data Bank (<http://www.rcsb.org/pdb>) in PDB format with resolution value 2.10 Å & R- values; free is 0.230 and R-value work is 0.189 represents that protein structure is best for docking analysis. The visualization of protein was done by AccelryBiovia Discovery 2017 R2 for cleaning ([www.advanceduninstaller.com/BIOVIA-Discovery](http://www.advanceduninstaller.com/BIOVIA-Discovery)).<sup>21</sup>

Prochek Ramachandran plot was used for the validation of target protein (2i54) defined by the phi ( $\phi$ ) and psi ( $\psi$ ) angles, the number of amino acid residues shown in the most favorable region is 90.8%, the additional allowed region is 8.9%, generously allowed regions are 0.3% and disallowed region is 0.0%. The number of amino acid residues was shown >90% which represents good quality of 3D model<sup>22</sup>. After validation of the protein, docking analysis was performed to find out protein-ligand interaction.<sup>23</sup>

## 2.2 Ligand preparation

I have downloaded 8500 drugs from the Zinc database approved by different regulatory agencies. It was visualized in the discovery studio visualization tool and saved in PDB format.<sup>24</sup> Open Babel was used for the energy minimization of ligands<sup>25</sup> and converted into pdbqt format with the help of a PyRx virtual screening tool for the protein-ligand interaction analysis.<sup>26</sup>

## 2.3 Virtual Screening and molecular docking

Virtual screening of 8500 drugs was done by AutoDock Vina PyRx 0.8 virtual screening tool against PMM (PDBID: - 2i54). The minimization of energy was carried out through open Babel PyRx 0.8 to get the stable and low energy conformation of the protein. AutoDock Vina version PyRx 0.8 tool was used for molecular docking of ligands on macromolecular protein (grid box i.e., xyz center value; x: 36.69, y: 6.52, z: 40.38 and dimensions in x: 57.36, y: 52.56, and z: 54.89). The analysis of docking is based on the Lamarckian Genetic Algorithm.<sup>27</sup> After that for each protein-ligand complex among the 9 poses, the best pose based on its conformation and binding affinity was selected and also obtained RMSD (Root Mean Square Deviation) values.<sup>28</sup> The RMSD values (UB/LB) zero refers to good interaction between protein and ligand. I have selected the top 46 ligands based on high binding energy and further molecular docking simulation was done through Schrodinger software (Desmond; maestro version 12.6.144 Schrodinger 2020-4 LLC, New York, USA) for validation.<sup>26</sup> **Table1**

The selected ligands were docked accordingly on the generated grid of the receptor using standard precision (SP) and OPLS3e force field to calculate their binding energy. Glide generated different conformations for the ligand-receptor interaction; the best pose was selected based on binding energy, hydrophobic interactions, hydrogen bonds, internal energy, root mean square deviation and desolvation. The result of protein and ligand complex structure was visualized in the discovery studio tool (Biovia).

### Table 1

## 2.4 Molecular dynamics simulation

The top lead drugs saquinavir (ZINC26664090) and grazoprevir (ZINC95551509) were selected and analyzed through molecular dynamics simulation at 100ns. The results have been evaluated with the help

of root mean square deviation (RMSD), root mean square fluctuation (RMSF), number of hydrogen bonds, hydrophobic interactions, ionic bonds and water bridges.

## 3. Results And Discussion

### 3.1 Virtual screening and binding interaction analysis

The library of 8500 drugs was downloaded from the Zinc database approved by different regulatory agencies (<https://www.fda.gov/>). Virtual screening was performed by PyRx virtual screening tool against PMM (PDBID: -2i54). Based on high binding affinity, chosen 46 drug molecules and molecular docking simulation was performed through Schrodinger software. **Table 1** The top 2 lead molecules (saquinavir and grazoprevir) were selected based on the best binding interaction between protein and ligand. Saquinavir and grazoprevir showed binding energy -10.144 and -10.131 kcal/mole respectively. Amphotericin B and Miltefosine were used as a standard drug and further analyzed through molecular dynamics simulation. The flow diagram of the work is given in **Fig. 1**. Top 2 lead molecules consist of different pharmacophoric groups including hydrogen bond acceptor (HBA), hydrogen bond donor (HBD), hydrophobic interaction, Pi alkyl, Salt bridge, Vander Waal interaction, pi-pi stacking etc. were visualized in the discovery studio.<sup>29</sup> The active site of amino acid residues involved in binding interaction of saquinavir were ASP187, ASN70, PHE11, GLY53, GLY54, VAL11, GLY212, VAL173, GLY174, GLY175, LYS208, ARG122, MET125, SER172, ASN214, ASP12, GLY45, ASP10, MRG2002, ASP180, ARG19, LYS50.<sup>30</sup> The saquinavir-PMM complex showed interactive forces such as Vander Waals, salt bridge, conventional hydrogen bond, carbon-hydrogen bond, metal acceptor, pi-anion, pialkyl. The active site of amino acid residues involved in binding interaction of grazoprevir were SER46, GLY174, ASP12, GLY44, PRO18, LYS188, ARG19, ASP207, VAL173, GLY213, GLY175, TRY216, GLU217, PHE182, ASP187, ASN70, MET125, MG2002, ASP180, ASN214, LYS208, SER172, ASP10, MG2002, ASP180, ARG112. The grazoprevir-PMM complex showed interactive forces such as Vander Waals, attractive charge, conventional hydrogen bond, carbon-hydrogen bond, metal acceptor, unfavorable acceptor-acceptor, pi- carbon, pi alkyl. Molecular dynamics simulation studies were performed to analyze the stability of saquinavir-2i54 and grazoprevir-2i54 complexes at 100ns. The MD simulations results have been evaluated with the help of root mean square deviation (RMSD), root mean square fluctuation (RMSF), the number of hydrogen bonds, hydrophobic interactions, ionic bonds, and water bridges.

**Table 2**

Interaction information from docking calculations between saquinavir and grazoprevir with PMM

Comp. Name/Zinc ID	Interacting amino acids	Applied forces
Saquinavir/ZINC26664090	ASP187, ASN70, PHE11, GLY53, GLY54, VAL11, GLY212, VAL173, GLY174, GLY175, LYS208, ARG122, MET125, SER172, ASN214, ASP12, GLY45, ASP10, MRG2002, ASP180, ARG19, LYS50	<ul style="list-style-type: none"> <li>• Van Der Waals</li> <li>• Salt bridge</li> <li>• Conventional hydrogen bond</li> <li>• Carbon hydrogen bond</li> <li>• Metal acceptor</li> <li>• Pi- anion</li> <li>• Pi alkyl</li> </ul>
Grazoprevir/ZINC95551509	SER46, GLY174, ASP12, GLY44, PRO18, LYS188, ARG19, ASP207, VAL173, GLY213, GLY175, TRY216, GLU217, PHE182, ASP187, ASN70, MET125, MG2002, ASP180, ASN214, LYS208, SER172, ASP10, MG2002, ASP180, ARG112	<ul style="list-style-type: none"> <li>• Van Der Waals</li> <li>• Attractive charge</li> <li>• Conventional hydrogen bond</li> <li>• Carbon hydrogen bond</li> <li>• Metal acceptor</li> <li>• Un favorable acceptor-acceptor</li> <li>• Pi- cation</li> <li>• Pi alkyl</li> </ul>

## 3.2 Molecular dynamics simulation studies:

MD simulation used to optimize and establish the stability of the protein-ligand complex. This study was performed by computing through the root mean square deviation (RMSD) and root mean square fluctuation of protein (RMSF) analysis of C $\alpha$ , ligand properties, the radius of gyration (rGy), molecular surface area (MolSA), solvent accessible surface area (SASA), polar surface area (PSA), hydrophobic bonds, ionic bonds and water bridges (**Table3**). The highest binding affinity of saquinavir/ZINC26664090 & grazoprevir/ZINC95551509-PMM complex was selected for MD simulation studies.

**Table 3**

### Molecular dynamics simulation studies of lead molecules

Parameters	2I54-ZINC000026664090	2I54-Grazoprevir
RMSD C $\alpha$ atoms (Å)	0.979-4.937	1.075-3.663
RMSD ligand fit on protein (Å)	1.582-4.935	1.935-5.655
RMSF C $\alpha$ atoms (Å)	0.690-5.526	0.498-3.835
rGyr (Å)	4.973-5.626	5.148-5.930
MolSA (Å <sup>2</sup> )	548.929-619.015	602.875-674.166
SASA (Å <sup>2</sup> )	171.793-372.838	316.886-669.971
PSA (Å <sup>2</sup> )	135.771-214.001	159.518-223.044
Hydrogen bonds	A: Arg19, A: Ser46, A: Asn127, A: Arg133, A: Gly174, A: Gln176, A: Ser178, Asp180, C: Pro165, C: Asp166, C: Gln168	A: Arg19, A: Lys50, A: Asn70, A: Arg122, A: Ser172, A: Val 173, A: Gly175, A: Gln176, A: Lys188, A: Gly212, A: Gly213, A: Asn214
Hydrophobic bonds	A: Arg122, A: Met125, A: Arg133, A: Ile177, A: Phe182 C: Lys184	A: Leu72, A: Arg122, A: Met125, A: Val173, A: Phe182, A: Lys188, A: Tyr216
Ionic bonds	A: Asp180	A: Asp12, A: Arg19, A: Lys50
Water bridges	A: Arg19, A: Gly45, A: Ser46, A: Lys50, A: Arg122, A: Asn127, A: Arg133, A: Ser172, A: Val173, A: Gly174, A: Gly175, A: Gln176, A: Ile177, A: Ser178, A: Asp180, C: Pro165, Asp166, C: Gln168	A: Asp12, A: Arg19, A: Gly45, A: Ser46, A: Asp47, A: Lys50, A: Glu69, A: Asn70, A: Arg122, A: Asn123, A: Arg133, A: Arg140, A: Tyr171, A: Ser172, A: Val173, A: Gly174, A: Gly175, A: Gln176, A: Asp180, A: Lys188, A: Lys208, A: Gly212, A: Gly213, A: Asn214

RMSD C $\alpha$  = Root mean square deviation of Protein, RMSD ligand = Root mean square deviation of ligand, RMSF C $\alpha$  = Root mean square fluctuation of protein, rGyr = Radius of Gyration, MolSA = Molecular Surface Area, SASA = Solvent Accessible Surface Area, PSA = Polar Surface Area

### 3.3 Estimation of complex stability *via* RMSD analysis

During MD simulation studies, RMSD is one of the most important parameters which gives complete information about the stability and insight into the structural conformation of the protein-ligand complex. The lower range of RMSD along with consistent variation throughout the simulation shows maximum stability of the protein-ligand complex. In the molecular dynamics simulation of saquinavir/ZINC26664090-2i54 & grazoprevir/ZINC95551509-2i54 complex, structural variations of C $\alpha$  atoms have first been individually determined for each point during the root mean square deviation (RMSD) analysis.

To calculate the RMSD value of the saquinavir-PMM complex from the starting to end of the simulation the RMSD of C $\alpha$  and saquinavir were varied from 0.979-4.937 Å and 1.582-4.935 Å [Figure 4A]. Saquinavir was shown the stability and bounded with protein throughout the simulation. But the protein was deviated from the stage of 2.10 to 4.11ns and again achieved the equilibrium point at the end of the simulation. Similarly, grazoprevir-complex also computed the RMSD of protein and ligand 1.075-3.663 Å and 1.935-5.655 Å [Figure 4B]. From the initially to 55 ns grazoprevir bound in the active site with rotational movements with the conformational changes but for some times 55.80 to 58.70 ns exhibited translational movement with the protein and again attained the equilibrium with the rotational movements in the binding pocket of protein. After analysing the RMSD values of both complexes which were demonstrated good stability against the target protein. Table 3

### 3.4 RMSF analysis

Root mean square fluctuation (RMSF) is measures the fluctuation in atoms of protein with the ligand during the MD simulation at a specific temperature and pressure. The RMSF values were analyzed 0.690-5.526 Å and 0.498-5.655 Å for saquinavir-2i54 and grazoprevir -2i54 complexes [Table 3]. Most of the fluctuations were noted in loop region in which Glu22, Gly212, and Asp245 amino acids of chain B with their RMSF 4.61 Å, 5.08 Å, and 5.526 Å in saquinavir-2i54 complex [Figure 4C]. Similarly, the fluctuations were examined Arg19, Pro112 with their RMSF 2.00 Å, 2.55 Å, and 3.83Å in the grazoprevir-complex [Figure 4D]. In grazoprevir-complex was analyzed less positional changes than saquinavir-2i54 during the 100ns molecular dynamics simulation. Table-3

### 3.5 Analysis of protein-ligand interaction and ligand properties

To calculate protein-ligand interaction, based on molecular docking results, the complexes which were displayed the lowest binding energies against the receptor were chosen. To check out the stability of respective complexes were performed MD simulation at 100ns in which hydrogen bond, hydrophobic interaction, ionic bond and water bridges were explored. As a result total of eleven hydrogen bonds (A: Arg19, A: Ser46, A: Asn127, A: Arg133, A: Gly174, A: Gln176, A: Ser178, Asp180, C: Pro165, C: Asp166, and C: Gln168) with amino acids, but out of these amino acids Asp180 involved 99% to form hydrogen bond with saquinavir, six hydrophobic interactions (A: Arg122, A: Met125, A: Arg133, A: Ile177, A: Phe182 C: Lys184) with interacting amino acids, one ionic bonds (A: Asp180) with amino acids and eighteen water bridges bond (A: Arg19, A: Gly45, A: Ser46, A: Lys50, A: Arg122, A: Asn127, A: Arg133, A: Ser172, A: Val173, A: Gly174, A: Gly175, A: Gln176, A: Ile177, A: Ser178, A: Asp180, C: Pro165, Asp166, C: Gln168) with amino acids for saquinavir/ZINC26664090-2i54complex Table 3. But, on the other hand, in grazoprevir-2i54 complex it is found that twelve hydrogen bonds (A: Arg19, A: Lys50, A: Asn70, A: Arg122, A: Ser172, A: Val 173, A: Gly175, A: Gln176, A: Lys188, A: Gly212, A: Gly213, A: Asn214), but out of these amino acids Gly212 involved 81% to formed hydrogen bond with grazoprevir, seven hydrophobic



interactions (A: Leu72, A: Arg122, A: Met125, A: Val173, A: Phe182, A: Lys188, A: Tyr216), three ionic bonds (A: Asp12, A: Arg19, A: Lys50) with amino acids and twenty-four water bridges (A: Asp12, A: Arg19, A: Gly45, A: Ser46, A: Asp47, A: Lys50, A: Glu69, A: Asn70, A: Arg122, A: Asn123, A: Arg133, A: Arg140, A: Tyr171, A: Ser172, A: Val173, A: Gly174, A: Gly175, A: Gln176, A: Asp180, A: Lys188, A: Lys208, A: Gly212, A: Gly213, A: Asn214) with amino acids were displayed<sup>31</sup> **Table 3**. Thus, based on these interactions, grazoprevir-2i54 and saquinavir-2i54 complexes were demonstrated magnificent stability and interactions throughout the simulations. (**Fig5 C-D**)

During the MD simulation of ZINC000026664090-2i54 and Grazoprevir-2i54, we have analysed that RMSD value of ZINC000026664090-2i54 ligand complex, the ligand was varied 0.6-2.10 Å with initial to 43.30ns and then achieved the equilibrium at 1.7Å with respect to reference conformation, radius of gyration measures the extendedness of ligand so the radius of gyration was noted that 4.973-5.626 Å at the end of simulation, molecular surface area (MolSA) of ligand was carried out 548.929-619.015 Å<sup>2</sup>, Solvent Accessible Surface Area (SASA) by water molecule 171.793-372.838 Å<sup>2</sup>, and Polar Surface area (PSA)135.771-214.001Å<sup>2</sup> which accessible in molecule by contributing oxygen and nitrogen atoms **Table 3**. Similarly, in Grazoprevir-2i54 the RMSD value of ligand was estimated that 1.00-2.54 Å with the respect to reference conformation, the radius of gyration (rGyr) in which estimated the stretchiness of ligand 5.148-5.930 Å, molecular surface area (MolSA) of ligand was evaluated 602.875-674.166 Å<sup>2</sup>, Solvent Accessible Surface Area (SASA) was 316.886-669.971 Å<sup>2</sup> in which the molecule accessible surface area by water molecule as well as polar surface area 159.518-223.044 Å<sup>2</sup> accessible of oxygen and nitrogen of the molecule in whole system**Table3**.

## 4. Conclusion

A drug repurposing study was carried out to find novel drugs against PMM (2i54). Thus, 8500 approved drugs from the Zinc data base were screened initially using a virtual screening tool and selected the top 46 drugs were based on a high binding score. The molecular docking simulation of the top 46 drugs was carried out by using the Glide module of Schrodinger software which hypothesized that grazoprevir and saquinavir could act as promising PMM (2i54) inhibitors. The results showed that the threshold binding affinity of saquinavir and grazoprevir are -10.144 and -10.131 kcal/mole for PMM (2i54) respectively. Further, we conducted the molecular dynamics simulation of both complexes saquinavir-2i54 and grazoprevir-2i54 for 100ns. In grazoprevir-2i54 complex, the RMSD values of ligand 1.075-3.663 Å with RMSF value of protein 0.498-3.835Å as well as the RMSD value of ligand in saquinavir-2i54 was noted that 0.979-4.937Å with RMSF value 0.690-5.526 Å of protein. Both complexes were exhibited a good stability in the binding pocket against the target receptor. Our work could provide new possibilities for the treatment of CL.

## Declarations

### Acknowledgment

The authors gratefully acknowledge the R&D wing of Integral University, Lucknow, for providing communication number IU/R&D/2021-MCN0001328.

## Declarations

Funding NA

## Conflicts of interest/Competing interests:

There is no conflict of interest.

## Availability of data and material

N/A

## Code availability

PyRx 0.8 virtual screening tool vina version 2.0., Desmond (maestro version 12.6.144 Schrodinger 2020-4 LLC, New York, USA

## Authors' contributions

All the authors are contributed to the manuscript.

## References

1. Félix Matadamas-Martínez, Alicia Hernández-Campos, Alfredo Téllez-Valencia, Alejandra Vázquez-Raygoza, Sandra Comparán-Alarcón, Lilián Yépez-Mulia, and Rafael Castillo, Leishmania mexicana Trypanothione Reductase Inhibitors: Computational and Biological Studies, *Molecules*:2019 ;24:3216. Doi;10.3390/molecules24183216
2. Juliana Ide Aoki, Sandra Marcia Muxel, Juliane Cristina Ribeiro Fernandes and Lucile Maria Floeter-Winter The Polyamine Pathway as a Potential Target for Leishmaniasis Chemotherapy, *Scientific Reports*; 2018; 75867. doi.org/10.5772/intechopen.75867.
3. Henry W Murray , Jonathan D Berman, Clive R Davies, Nancy G Saravia, Advances in leishmaniasis, *Lancet*. 2005 Oct 29-Nov 4;366(9496):1561-77.
4. Saker L et al. Globalization and infectious diseases: a review of the linkages. UNICEF/UNDP/World Bank/WHO Special Programme for Research and Training in Tropical Diseases. TDR/STR/SEB/ST/04.2. Geneva, World Health Organization, 2004.
5. WHO report 2021, <https://www.who.int/.../data/themes/topics/topic-details/GHO/leishmaniasis>.
6. Aronov, A. M., Suresh, S., Buckner, F. S., Van Voorhis, W. C., Verlinde, C. L., Opperdoes, F. R., et al. (1999). Structure-based design of submicromolar, biologically active inhibitors of trypanosomatid glyceraldehyde-3-phosphate dehydrogenase. *Proc. Natl. Acad. Sci. U.S.A.* 96, 4273–4278. doi: 10.1073/pnas.96.8.4273

7. Chowdhury, S. F., Villamor, V. B., Guerrero, R. H., Leal, I., Brun, R., Croft, S. L., et al. (1999). Design, synthesis, and evaluation of inhibitors of trypanosomal and leishmanial dihydrofolate reductase. *J. Med. Chem.* 42, 4300–4312. doi: 10.1021/jm981130+
8. Verlinde, C. L., Hannaert, V., Blonski, C., Willson, M., Périé, J. J., Fothergill, Gilmore, L. A., et al. (2001). Glycolysis as a target for the design of new anti-trypanosome drugs. *Drug Resist. Updat.* 4, 50–65. doi: 10.1054/drup.2000.0177
9. Olin-Sandoval, V., Moreno-Sanchez, R., and Saavedra, E. (2010). Targeting trypanothione metabolism in trypanosomatid parasites. *Curr. Drug Targets* 11, 1614–1630. doi: 10.2174/1389450111009011614
10. Descoteaux, A., Luo, Y., Turco, S. J., and Beverley, S. M. (1995). A specialized pathway affecting virulence glycoconjugates of *Leishmania*. *Science* 269, 1869–1872. doi: 10.1126/science.7569927
11. Descoteaux, A., and Turco, S. J. (1999). Glycoconjugates in *Leishmania* infectivity. *Biochim. Biophys. Acta* 1455, 341–352. doi: 10.1016/S0925-4439(99)00065-4
12. Podinovskaia, M., and Descoteaux, A. (2015). *Leishmania* and the macrophage: a multifaceted interaction. *Future Microbiol.* 10, 111–129. doi: 10.2217/fmb.14.103
13. Lamotte, S., Späth, G. F., Rachidi, N., and Prina, E. (2017). The enemy within: targeting host-parasite interaction for antileishmanial drug discovery. *PLoS Negl. Trop. Dis.* 11:e0005480. doi: 10.1371/journal.pntd.0005480
14. Pomel, S., and Loiseau, P. M. (2013). “GDP-mannose: a key-point for target identification and drug design in kinetoplastids,” in *Trypanosomatid Diseases: Molecular Routes to Drug Discoveries*, eds T. Jäger, O. Koch, and L. Flohe (Weinheim: Wiley-VCH Verlag GmbH and Co. KGaA), 315–334.
15. Varki, A. (2007). Glycan-based interactions involving vertebrate sialic-acid recognizing proteins. *Nature* 446, 1023–1029. doi: 10.1038/nature05816
16. Colley, K. J., Varki, A., and Kinoshita, T. (2017). “Chapter 4: cellular organization of glycosylation,” in *Essentials in Glycobiology*, 3rd Edn., eds A. Varki, R. D. Cummings, J. D. Esko, P. Stanley, G. W. Hart, M. Aebi, et al. (New York, NY: Cold Spring Harbor Laboratory Press), 41–49.
17. Wei Mao<sup>1</sup>, Pierre Daligaux, Nouredine Lazar, Tâp Ha-Duong, Christian Cavé, Herman van Tilbeurgh, Philippe M. Loiseau<sup>1</sup> & Sébastien Pomel. Biochemical analysis of leishmanial and human GDP-Mannose Pyrophosphorylases and selection of inhibitors as new leads. *scientific reports* ; 2017 Apr 7;7(1):751. doi:10.1038/s41598-017-00848-8.
18. Pomel, S., Rodrigo, J., Hendra, F., Cavé, C., and Loiseau, P. M. (2012). In silico analysis of a therapeutic target in *Leishmania infantum*: the guanosine-diphospho-D-mannose pyrophosphorylase. *Parasite* 19, 63–70. doi: 10.1051/parasite/2012191063
19. J.L. Weisman, A.P.Liou, A.A.Shelat, F.E. Cohen, R.K. Guy, J.L.DeRisi, Searching for new antimalarial therapeutics amongst known drugs, *Chem Biol Drug Des.* 67 (2006) 409–416.
20. C.R. Chong, D.J. Jr Sullivan, New uses for old drugs, *Nature*448 (2007) 645–646.

21. Sébastien Pomel\*, Wei Mao, Tâp Ha-Duong, Christian Cavé and Philippe M. Loiseau. GDP-Mannose Pyrophosphorylase: A Biologically Validated Target for Drug Development Against Leishmaniasis. *Microbiol. Front. Cell. Infect. Microbiol.*; 2019; May 9:186. doi.org/10.3389/fcimb.2019.00186
22. D.K. Rai, E. Rieder, Homology modeling and analysis of structure predictions of the bovine rhinitis B virus RNA dependent RNA polymerase (RdRp), *Int. J. Mol. sci.* 13 (2012) 8998-9013.
23. R.R.Deshpande, A.P.Tiwari, N.Nyayanit, M. Modak, *In silico* molecular docking analysis for repurposing therapeutics against multiple proteins from SARS-CoV-2, *Eur J Pharmacol.* 886 (2020) 173430.
24. Irwin, J. & Shoichet, B. ZINC—a free database of commercially available compounds for virtual screening. *J. Chem. Inf. Model:* 2005; 45, 177–182, doi.org/10.1021/ci049714
25. Trott O, Olson AJ, AutoDock Vina: improving the speed and accuracy of docking with a new scoring function, efficient optimization, and multithreading. *J Comput Chem* 2010; 31:455–461.
26. Madhu SudhanaSaddala, Pradeep Kiran Jangampalli Adi and Usha Rani A, In Silico Drug Design and Molecular Docking Studies of Potent Inhibitors against Cathepsin-L (CtSl) for Sars Disease. *Journal of Research and Development*; 2016; 4:2: 0145. doi: 10.4172/2311-3278.1000145.
27. Boxin Guan, Changsheng Zhang, and Yuhai Zhao, HIGA: A Running History Information Guided Genetic Algorithm for Protein–Ligand Docking, *Molecules.* 2017 Dec; 22(12): 2233.
28. S.Singh, H.Florez, Coronavirus disease 2019 drug discovery through molecular docking, *F1000Res.* 9 (2020) 502.
29. P.Shukla, R.Khandelwal, D.Sharma,A.Dhar , A. Nayarisseri, S.K.Singh, Virtual Screening of IL-6 Inhibitors for Idiopathic Arthritis,*Bioinformatics*15 (2019) 121–130.
30. MF. Khan, MA. Khan,ZA. Khan, T. Ahamad,WA. Ansari, In-silico Study to Identify Dietary Molecules as Potential SARS-CoV-2 Agents, *Letters in Drug Design & Discovery* 2021; 18(6). <https://dx.doi.org/10.2174/1570180817999201209204153>
31. WA. Ansari, T. Ahamad, MA. Khan, ZA. Khan,MF. Khan. Exploration of Luteolin as Potential Anti-COVID-19 Agent: Molecular Docking, Molecular Dynamic Simulation, ADMET and DFT Analysis, *Letters in Drug Design & Discovery* 2022; 19. <https://dx.doi.org/10.2174/1570180819666211222151725>

## Table

Table 1 is available in the Supplementary Files section

## Figures

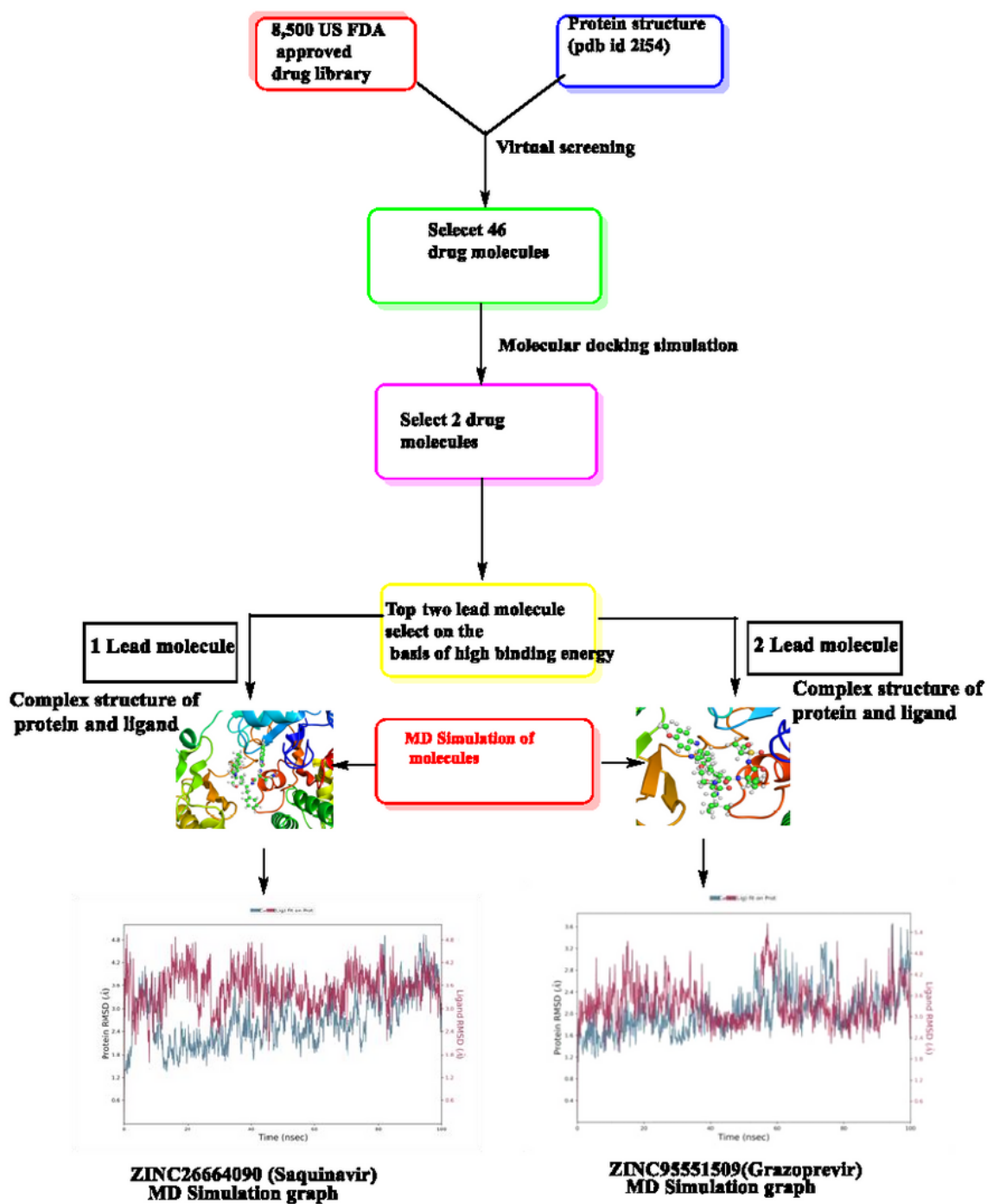
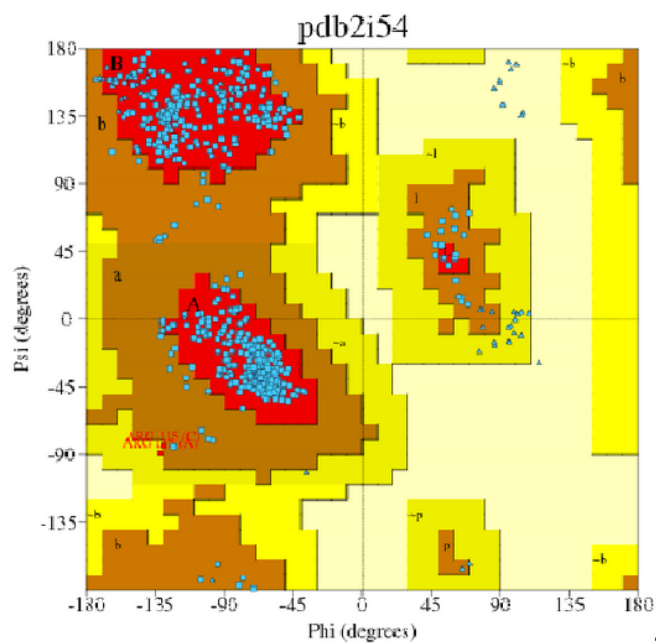


Figure 1

Graphical representation of virtual screening, molecular docking and MD simulation studies



### Procheck Statistics

	No. of residue	%age
Most favoured regions [A,B,L]	583	90.8%
Additional allowed regions [a,b,l,p]	57	8.9%
Generously allowed regions [~a,~b,~l,~p]	2	0.3%
Disallowed regions[XX]	0	0.0%
Non-glycine and non-proline residues	642	100.0%
End-residues (excl. Gly and Pro)	6	
Glycine residues	57	
Proline residues	21	
Total number of residues	726	

Figure 2

Ramachandran Plot

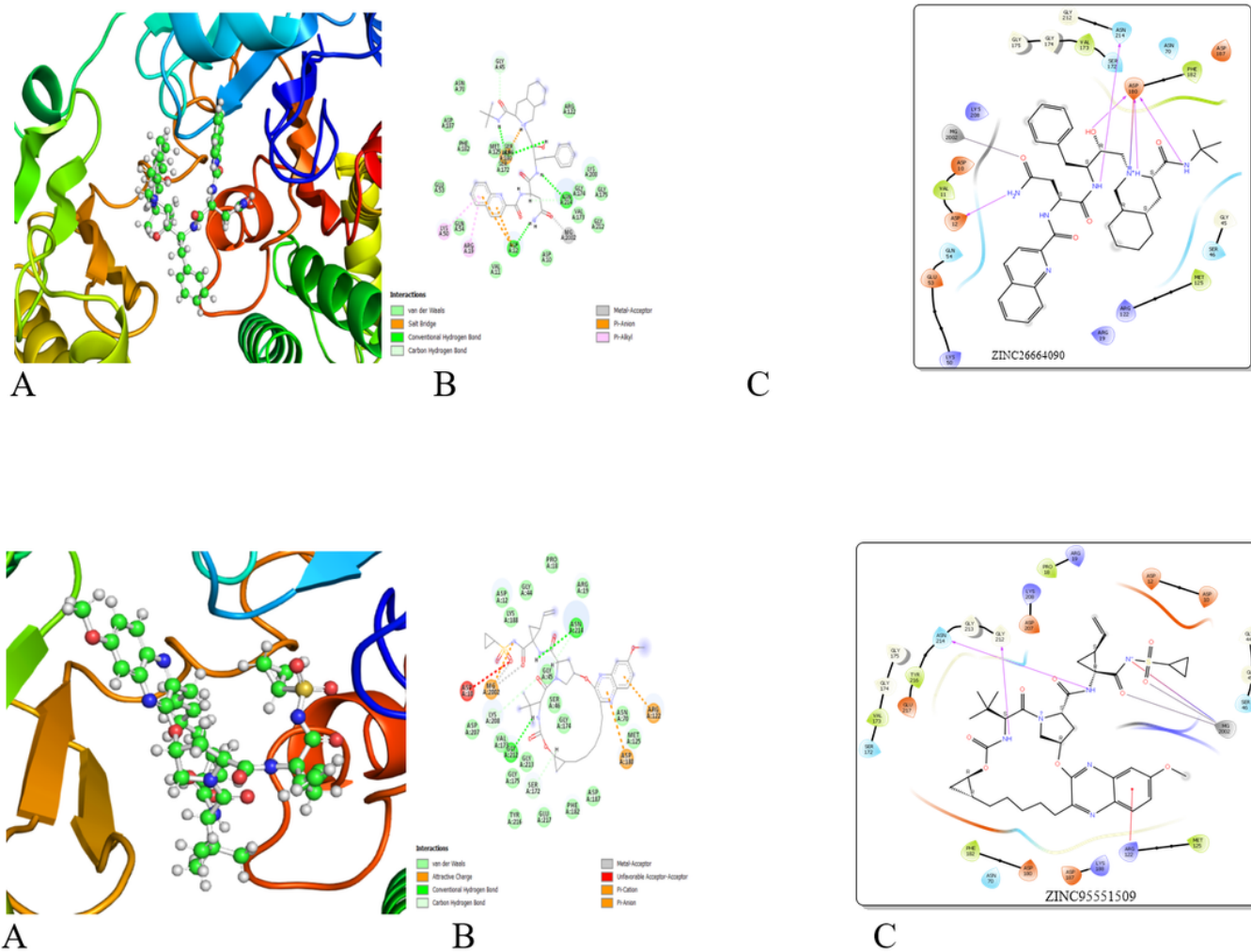


**Figure 3**

Interaction details of **ZINC26664090** (Saquinavir) and **ZINC95551509** (Grazoprevir) through 3D and 2D structure.

A: 3D Complex structure of **ZINC26664090** (Saquinavir) with protein Phosphomannomutase (2i54 pdb id) shown docking poses, B: Applied interaction forces in protein and ligand, C: 2D structure of **ZINC26664090** with protein Structure (2i54 pdb id)

A: 3D Complex structure of **ZINC95551509** (Grazoprevir) with protein Structure (2i54 pdb id) shown docking poses, B: Applied interaction forces in protein and ligand, C: 2D structure of **ZINC95551509** with protein Structure (2i54 pdb id).



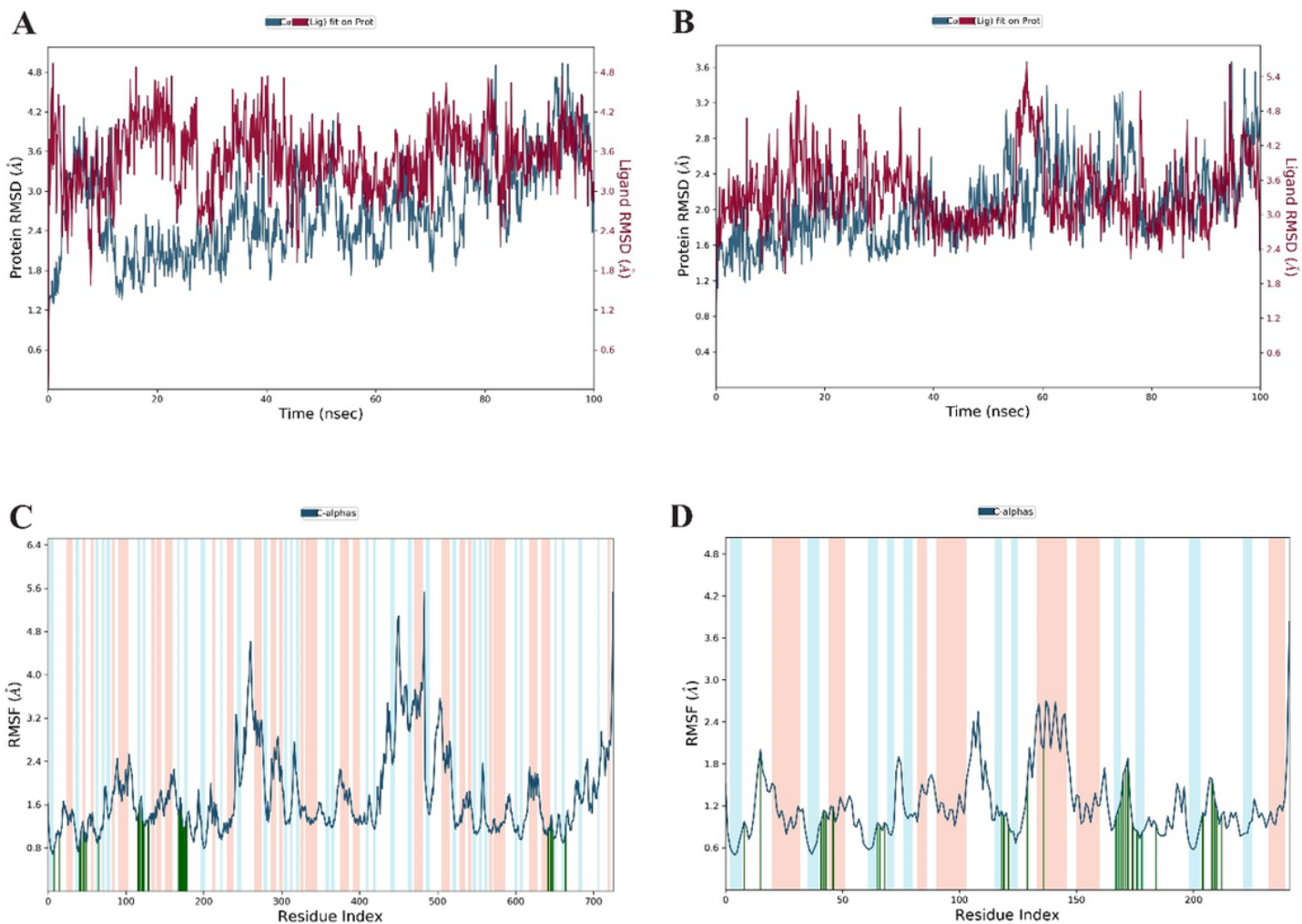


**Figure 4**

(A-B) RMSD graph of Saquinavir-2i54 and Grazoprevir-2i54 complex. (C-D) RMSF graph of saquinavir-2i54 and grazoprevir-2i54 complex during 100 ns molecular dynamicssimulation.



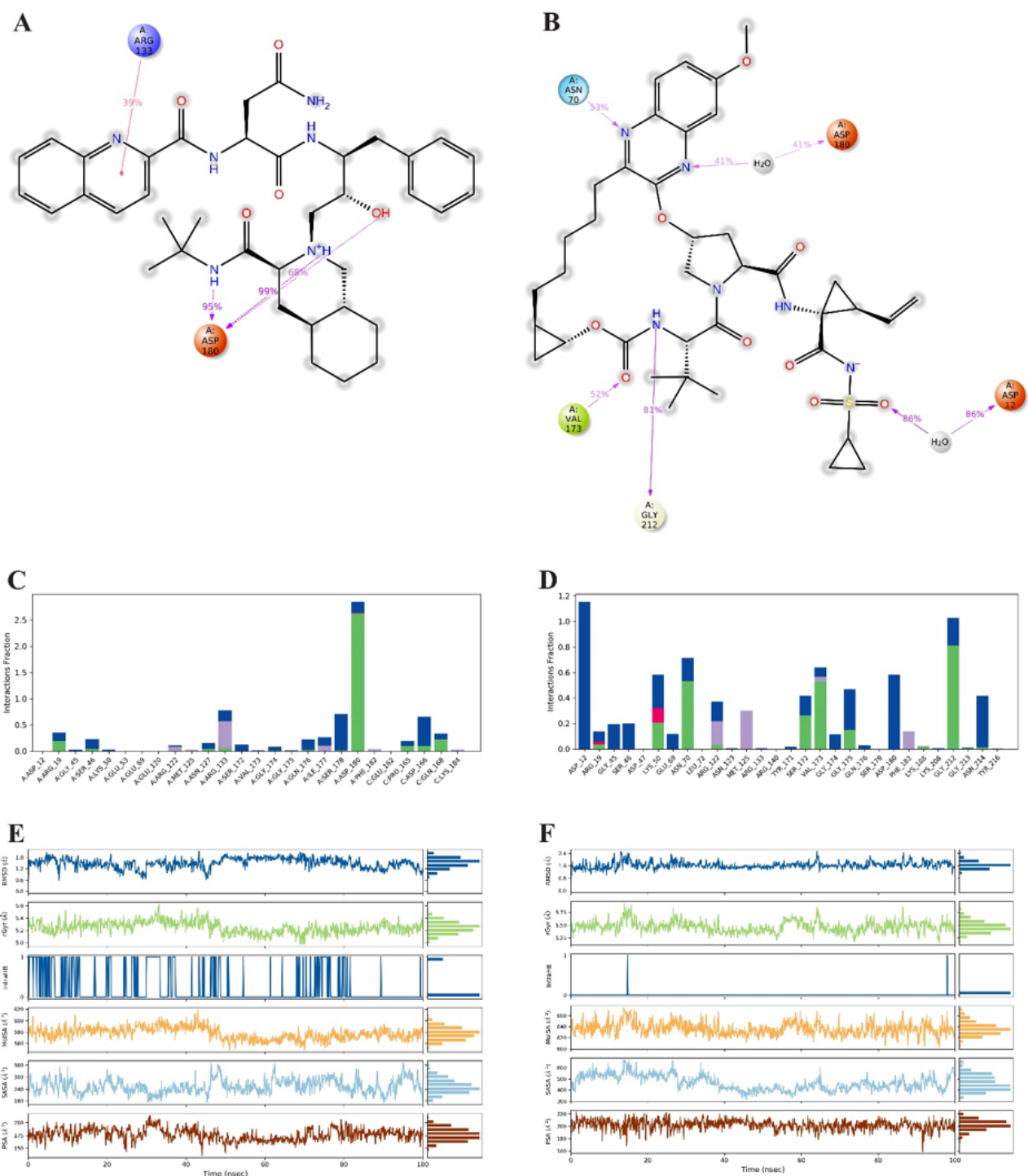


**Figure 5**

(A-B) 2D-structure of Saquinavir and Grazoprevir interaction with 2i54receptor.(C-D) In histogram displayed the bond interaction with amino acids during 100ns molecular dynamics simulation. (E-F) Ligand contact properties *viz.* RMSD (Blue Line), Radius of Gyration (Green Line), Molecular Surface Area (Orange line), Solvent Accessible Surface Area (Cyan blue line), and Polar Surface Area (Brown line).

## Supplementary Files

This is a list of supplementary files associated with this preprint. Click to download.

- [RevisedGraphicalabstract.docx](#)
- [RevisedSupplementarydata.docx](#)
- [Table1.docx](#)